MICROWAVE SYNTHESIS OF SILVER-GRAPHENE OXIDE FOR DETERMINATION OF MERCURY ION (Hg^{2+})

by

NOR SYAHIRAH BINTI SAMSUDDIN

A thesis submitted in fulfilment of the requirement for the degree of Bachelor of Applied Science (Materials Technology) with honours.

FACULTY OF EARTH SCIENCE
UNIVERSITI MALAYSIA KELANTAN

2017

DECLARATION

I declare that this thesis entitled MICROWAVE SYNTHESIS OF SILVER-GRAPHENE OXIDE FOR DETERMINATION OF MERCURY ION (Hg^{2+}) is the result of my own research except as cited in the references. The thesis has not been accepted for any degree and is not concurrently submitted in candidature of any other degree.

Signature : _____

Name : Nor Syahirah Binti Samsuddin

Date : 3 January 2017

ACKNOWLEDGEMENTS

Foremost, I would like to take this opportunity to express my gratitude to Mr. An' Amt Bin Mohamed Noor as my supervisor for sharing his knowledge in synthesising graphene oxide to be used in optical application. He supports me and provide me with useful suggestions, advice, knowledge and materials throught my thesis completion. His continuous support, discussions, comments and advices were the instrumental success of my final year project. I would like to thank Universiti Malaysia Kelantan who provides me the laboratory and equipment to finish my study, that able me to complete my final year project

Secondly, I would like to thank all the lab assistants in University Malaysia Kelantan for guiding me at the beginning phase of this final year project, especially in handling machines and equipment. They showed their dedication and responsibility in helping me to conduct the experiment.

I would like to thank my fellow lab mate, Nurul Afiqah Binti Mohd Mokhtar for the experiment discussions, for the sleepless night we were working together before the deadlines, and for all the fun we had in the last four years. I also want to thank my best friends in University Malaysia Kelantan, Syuhada and Adillah as they were always willing to help and give their best suggestions.

Finally, to my caring, loving, supportive parents Samsuddin Bin Hamat and Rohaniza Binti Ismail for supporting me spiritually throughout my life. To my best friend, Muhammad Nabil bin Mihat, thank you for your encouragement and support throughout this journey to complete my research.

MICROWAVE SYNTHESIS OF SILVER-GRAPHENE OXIDE FOR DETERMINATION OF MERCURY ION (Hg^{2+})

ABSTRACT

In this study, silver-graphene oxide were synthesized using microwave irradiation for the determination of mercury ion (Hg^{2+}) using spectrophotometry. Due to the harmful effects of Hg^{2+}, it is crucial to be able to detect and measure the level of Hg^{2+}. The GO-Ag nanocomposite are chosen as an assay for optical determination of Hg^{2+}. GO serve as an effective host material for the growth of Ag NPs due to the presence of surface functional groups and high specific surface area. A microwave-assisted method had been reported for the synthesis of Ag NP since it is well known as a rapid process in producing metallic nanoparticles, for example, gold, platinum, and palladium. Microwave synthesis only requires lower energy consumption compared to conventional heating method. The nanocomposite was characterized by UV-visible absorption spectra, X-Ray Diffraction (XRD), Fourier Transform Infrared Spectroscopy (FTIR) and Transmission Electron Microscopy (TEM). The color change of dark brown nanocomposite were observed during the determination of Hg^{2+} and it can be seen with bare eyes. Silver nanoparticle with narrow size distribution were formed under microwave irradiation and it were randomly distributed on the surface on graphene oxide. The FTIR analysis result showed the GO was partially reduced during the synthesis of GO-Ag. XRD analysis of GO-Ag shows the existence of AgNP on the graphene sheets with the diffraction pattern of silver crystal structure.

SINTESIS GELOMBANG MIKRO UNTUK PERAK GRAFEN OKSIDA BAGI PENENTUAN ION MERKURI

ABSTRAK

Dalam kajian ini, perak grafen oksida di sintesis menggunakan kaedah gelombang mikro untuk penentuan ion merkuri menggunakan alat spektrofotometri. Disebabkan oleh kesan merbahaya yang muncul dari ion merkuri, ia adalah sangat penting bagi mengesan dan mengukur paras ion merkuri. Nanokomposit perak grafen oksida dipilih sebagai cerakin untuk penentuan optik ion merkuri. Grafen oksida bertindak sebagai perumah yang efektif untuk pertumbuhan partikel nano perak disebabkan kehadiran fungsi kumpulan dan permukaan kawasan yang tinggi. Kaedah gelombang mikro dilaporkan untuk sintesis partikel nano perak disebabkan ia terkenal sebagai proses yang cepat dalam menghasilkan partikel nano metalik, contohnya emas, platinum dan palladium. Sintesis gelombang mikro hanya menggunakan tenaga yang sedikit berbanding kaedah pemanasan konvensional. Komposit nano telah dicirikan menggunakan UV-vis penyerapan spectrum (*UV-vis*), Belauan Sinar X (*XRD*), Spektroskopi Inframerah Transformasi (*FTIR*) dan Mikroskop Elekron Pancaran (*TEM*). Perubahan ke atas warna coklat gelap diperhatikan semasa penentuan ion merkuri dan dapat dilihat dengan mata kasar. Partikel nano perak dengan pengagihan saiz yang sempit terbentuk disebabkan oleh sintesis gelombang mikro dan ia diagihkan secara rawak diatas permukaan grafen oksida. Keputusan analisis FTIR menunjukkan pengurangan grafen oksida secara separa ketika sintesis perak grafen oksida. Analisis XRD perak grafen oksida menunjukkan kewujudan partikel nano perak di atas permukaan grafen dengan mempunyai pesongan corak untuk struktur kristal perak.

TABLE OF CONTENTS

LIST OF FIGURES

LIST OF ABBREVIATIONS

CVD	Chemical vapour deposition
HOPG	Highly oriented pyrolytic graphite
AgHg	Silver amalgams
CNT	Carbon nanotubes
GFN	Graphene family nanotubes
FLG	Few layer graphene
PECVD	Plasma enhanced CVD
LB	Langmuir-Blodgett
SW	Stone-Wales
DSSC	Dye-sensitived solar cell
RGO	Reduced graphene oxide
GO	Graphene oxide
AgNPs	Silver nanoparticles
SEM	Scanning Electron Microscope
TEM	Transmission Electron Microscope
XRD	X-Ray Diffraction
FTIR	Fourier Transform Infrared Spectroscopy
UV-vis	Ultraviolet-Visible Spectroscopy

LIST OF SYMBOLS

ml	milliliter
$Wm^{-1}K^{-1}$	Thermal conductivity
cm^2/Vs	Mobility of electron
µL	microliter
mM	millimolar
kV	kilovolt
nm	nanometer

CHAPTER 1

INTRODUCTION

1.1 Background of Study

Graphene consist a single layer of atomic carbon and exist as a two dimensional monoatomic thick building block of a carbon allotrope in a honeycomb lattice (Singh *et al.,* 2011). Graphene exhibits properties that are useful in various field of application. For an instance, it has high mobility of electron at room temperature (250, 000 / Vs, exceptional thermal conductivity (5000 W and exhibit superior mechanical properties with Young's Modulus of 1 TPa, high fracture strength (125 GPa) and super charge carrier mobility (Singh *et al.,* 2011; Xia *et al.,* 2015). This 2-D material possess an electrically and thermally conductive and transparent material, which leads to the unusual quantum Hall Effect (Royal *et al*., 2010). The structural flexibility of graphene is reflected in its electronic properties (Neto, 2009). Graphene consist of unusual charge carriers that resulting in massless relativistic particles behaviour, called Dirac Fermions behaviour (Royal *et al*., 2010). Its potential application including, supercapacitors, biosensors, field emission cathode, organic photovoltaic, catalysts and touch panels (Silwana *et al.,* 2015).

Various method are used to synthesis graphene. Graphene is obtained from graphite. The synthesis methods, are exfoliation and cleavage, chemical vapour deposition (CVD), thermal decomposition, chemical and electrochemical reduction (Nersisyan *et al.,* 2014; Royal *et al.,* 2010).

Silver nanoparticles (AgNPs) has attracted much attention due to its high catalytic activity, electronic and optical properties (Chung *et al.,* 2016). To enhance the AgNPs ability it can be done by deposit onto reduced graphene oxide (RGO) layer to produce highly dispersed nanoparticles which enhanced the active surface area. as an optical sensor for mercury (Hg^{2+}) ion. Due to the contamination of the environment with the heavy metal, the optical sensor for the detection Hg^{2+} ion is crucial. As a unique feature, mercury atoms can complex with silver metal to form silver amalgams (AgHg). Beside, amalgam AgHg attracted a lot of interest with respect to the electronic and optical properties of the bimetallic structure. In the past few years, silver amalgam electrodes are intensively sought to substitute the convenient mercury electrode material for electrochemical detections of various targets from proteins and DNAs, to small molecules and metal ions (Deng *et al.,* 2013).

1.1 Problem Statement

There are many methods to synthesis graphene that can be done, however it still depends on the quality of the final product and applications purposes. Graphene can be synthesized by various methods such as chemical vapour deposition (CVD), mechanical exfoliation and cleavage, and annealing a single-crystal SiC under ultrahigh vacuum. However, these methods have many disadvantages including high energy requirement, low yield, and limitation of instrument and requires certain specialise to run the experiment (Loryuenyong *et al.,* 2013). In the other hand, RGO was modified with different materials such as polymers, inorganic nanoparticles and biomaterials in the process reduction of nanoparticle-graphene oxide (GO) nanocomposite, which can also endow RGO extra excellent property (Yujie Han *et*

al., 2013). Ag was chosen because of its low cost compared to Au (Kai-Chih Hsu, 2014), non-toxic and easy to handle.

In this experiment, simplified Hummers Method is used to produce graphene oxide (GO). The chemical method has become a promising route to produce reduced graphene oxide (RGO) sheets, although RGO derived by this method could contain a significant amount of oxygen functional groups and defects. This is because it is simple, inexpensive, and suitable for large-scale or mass production. Previous works have reported the reduction by using reducing agent such as hydrazine hydrate, ammonia, $NaBH_4$ and formaldehyde. However, these chemicals might be highly toxic to human and environment (Loryuenyong *et al.*, 2013). A microwave-assisted method had been reported for the synthesis of AgNP, since it is well known as a rapid process in producing metallic nanoparticles, for example, gold, platinum, and palladium. Microwave-assisted synthesis is used because it only require lower energy consumption compared to conventional heating method (Chook *et al.*, 2012).

1.2 Objectives

1. To synthesis GO using simplified Hummers Method.

2. To synthesis GO-Ag nanocomposite using microwave irradiation.

3. To study the application of GO-Ag in optical sensors for the detection of Hg^{2+} ion.

1.4 Expected Outcome

The GO and silver-GO will be obtained via simplified Hummers Method and reduction by microwave method respectively. The size of GO will exceed micrometer size and the AgNPs will homogenously decorated onto the GO layer.

The GO-Ag obtained will show high limit of detection for the determination of Hg^{2+} ion and can be seen with the bare eyes.

CHAPTER 2

LITERATURE REVIEW

2.1 Allotropes of Carbon

Carbon is the base for DNA and all life on Earth, in which carbon are exist in many forms. The most common form of carbon is graphite. Graphite consist of stacked sheets of carbon with a hexagonal structure. Diamond will formed when it is put under high pressure. Diamond is the metastable form of carbon. A new form of carbon are called Fullerenes. Fullerenes consist of 60 carbon atoms and are made up of 20 hexagons and 12 pentagons and led to the formation of sphere. Carbon nanotubes (CNT), is a related quasi-one-dimensional form of carbon. CNT can be formed from graphene sheets which are rolled up to form tubes, and their ends are half spherical as in the fullerenes (see Figure 2.1). This metallic single walled nanotubes has many similarities with graphene, as it exhibits the same electronic and mechanical properties (Royal *et al.*, 2010).

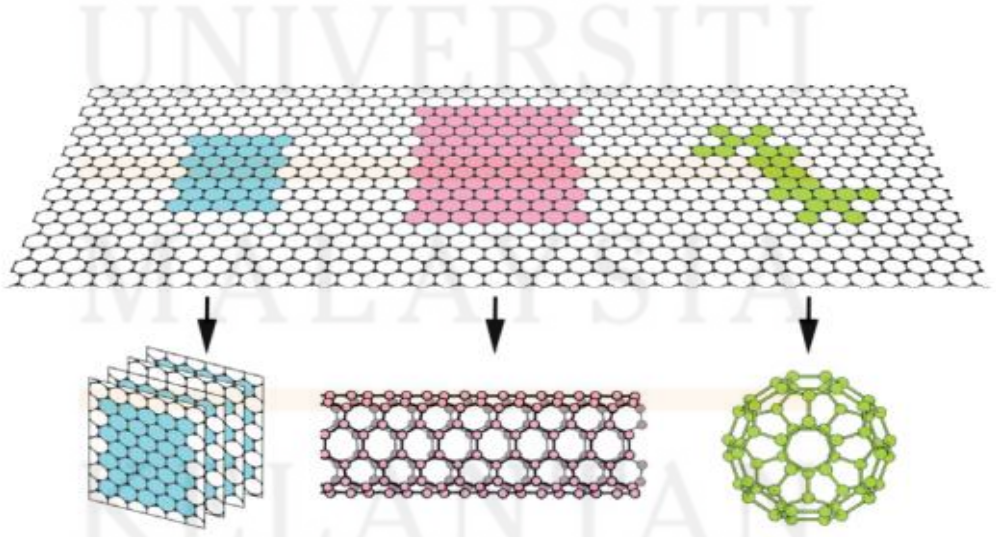

Figure 2.1: Graphite, nanotube and fullerene as derivatives of graphene (Ismagilov, 2013).

Graphene is a single layer of carbon packed in a hexagonal (Honeycomb) lattice, with a carbon-carbon distance of 0.142 nm (Royal *et al.,* 2010). Its special structure of monolayer graphite endows it with many excellent properties such as good chemical stability, high Quantum Hall effect and extraordinary electronic transport properties (Fu *et al.,* 2013). Graphene is a basic building block for graphitic materials for all dimensionalities. It is a material that has experienced a tremendous increase in the last few years, which has the possibilities to substitutes for rare earth metal (Thondaiman, 2015). Graphene exhibits great ability for potential application in the fields of nanoelectronics, sensors, batteries, super-capacitors, hydrogen storage and nanocomposite (Han *et al.,* 2016). For example, graphene can be used to create good capacitor when either combined with a polymer as a composite or used in its pure form. Graphene has also been used to construct sensitive sensors that can detect very low traces of a specific prostrate antigen (Thondaiman, 2015).

GO consist of single atom thick layer of graphene sheets. It is a highly oxidised form of chemically modified graphene. GO can be dissolved in water and various solvents because GO bears some functional groups (Gao *et al.,* 2014). GO exhibit a high defect density on its physical properties due to the additional functional groups on it. Both RGO and GO has different structural properties. RGO possess a better crystal structure than GO. GO, RGO and graphene exhibits a different properties from each other (Zhang *et al.,* 2015). Both GO and RGO possess unique properties that differ from those of pristine graphite because of the structural changes that arise from the oxygen functionalities into the bonded carbon network (Drewniak *et al.,* 2016). The techniques applied for the preparation of GO and its further reduction to reduced graphene oxide affect the properties of these materials, due to the presence of additional functional groups. GO contains, among others,

many hydroxyl, carboxyl and epoxy groups (Drewniak *et al.*, 2016). GO, consisting of a single atom thick layer of graphene sheets with carboxylic acid, epoxide and hydroxyl groups in the plane, is a highly oxidized form of chemically modified graphene (Zhang *et al.*, 2015). GO has been widely used as starting materials for the synthesis of processible graphene (Fu *et al.*, 2013). They are applied in a variety of civil, mechanical and aerospace applications. RGO is often preferred as graphene substitute owing to its scalable preparation through GO and facile functionalization for coupling with different substances (Papailias *et al.*, 2015). RGO can greatly improve tribological and mechanical performance of composite (Chen *et al.*, 2016). Compared to two dimensional assembly of graphene (like in bucky papers), 3D graphene-based materials exhibit advantages, such as large surface area, high porosity and different physical and electronic properties (Sridhar *et al.*, 2013). Graphene not only enables to modify mechanical properties of polymer matrix, but also provides additional high electrical and thermal conductivity, and carbonaceous materials are attractive in the design of lighter and tougher composite materials (Wang *et al.*, 2016).

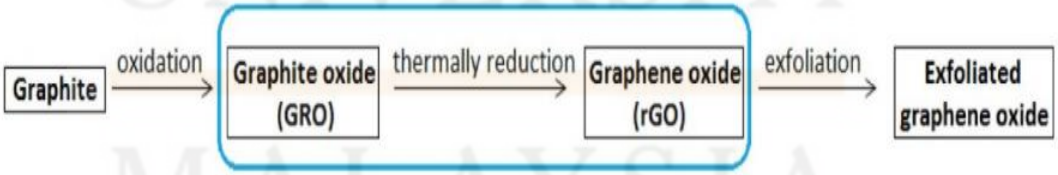

Figure 2.2: Preparation of graphite oxide and graphene oxide (Drewniak *et al.*, 2016).

2.2 Synthesis of Graphene

Graphene can be synthesised using various method, for example by chemical vapour deposition (CVD), thermal decomposition and mechanical exfoliation and cleavage.

2.2.1 Chemical Vapor Deposition

Chemical vapour deposition (CVD) can be divided into Thermal CVD and Plasma Enhanced CVD.

2.2.1.1 Thermal CVD

CVD technique is the most suitable technique for large scale production of mono- or few- layer graphene films. Chemical vapour deposition (CVD) from hydrocarbon precursors deposited on metals catalyst like nickel (Ni) or copper (Cu) is so far the most promising technique for large-area graphene growth. Ni which forms a buffer layer for graphene growth has an advantage over Cu because the graphene can be grown at lower temperature (Othman *et al.*, 2015). Carbon is dissolve in the nickel substrates and then continue by a precipitation of carbon on the substrate by cooling the Nickel. Then the next step is to place the nickel substrate in a CVD chamber at a vacuum of 10^{-3} Torr and temperature below 1000ºC with a dilute hydrocarbon gas (Singh *et al.*, 2011). Porous silicon is considered as an ideal substrate for controlled growth of carbon nanotubes (Garima, 2014). An interesting feature of the CVD approach to synthesize graphene is the possibility for substitution doping by introducing other gases, such as NH_3, during the growth. The nitrogen atom can be doped into graphene as *pyridinic*, *graphitic* and *pyrrolic* forms (Singh *et al.*, 2011). This process only consume a low cost and have the potential to enable several large area applications of graphene in the future. However, the disadvantages of CVD technique including, the difficulty to control the process, thickness and

quality of graphene may be affected due to the different cooling rates and also the graphene growth is self-limiting (Avouris & Dimitrakopoulos, 2012). CVD process will damage the electrical conductivity of graphene due to the disruption of the network of sp^2 carbon bonds in the graphene sheets (Vermisoglou *et al.*, 2015).

2.2.1.2 Plasma Enhanced CVD

Plasma Enhanced CVD (PECVD) is alternatively used to promote graphene growth rate at relatively lower temperature and have been widely used in the synthesis or functionalization of carbon nanomaterial, such as graphene (Fan *et al.*, 2015; Othman *et al.*, 2015). During the fabrication of nanostructured graphite-like carbon using a dc discharge PECVD, thick graphite structured is obtained. The advantages of this technique are very short deposition time (<5 min) and a lower growth temperature, which is 650˚C compared to thermal CVD method, which is 1000˚C (Singh *et al.*, 2011). However, Plasma Enhanced CVD produce lower quality graphene films compared to Thermal CVD (Jr & Sheehan, 2014).

2.2.1.3 Thermal Decomposition on SiC and other Substrates

Products obtained on SiC substrates require no transfer before processing devices. When SiC substrate is heated under UHV, silicon atoms sublimate from the substrate. The removal of Si leaves surface carbon atoms to rearrange into graphene layers. The thickness of graphene layers depends on the annealing time and temperature. The formation of few-layer graphene (FLG) typically requires few minutes annealing of the SiC surface at temperature around 1200˚C. Vapour phase annealing has been used to produce FLG on SiC. This method leads to the formation of FLG on SiC with an improved thickness homogeneity. Although producing graphene on SiC substrates is attractive, several problems prevent the real

application. For example, it is difficult to control the thickness of graphene layers in the routine production of large area graphene and the different of epitaxial growth patterns on different SiC polar face which could affect the physical and electronic properties of epitaxial graphene (Singh *et al.,* 2011).

2.2.2 Exfoliation and Cleavage

Exfoliation and cleavage involve mechanical exfoliation of graphene in solutions, and mechanical exfoliation of graphene using HOPG sheets.

2.2.2.1 Mechanical Exfoliation in Solutions

Mechanical exfoliation is a simple peeling process. Highly oriented pyrolytic graphite (HOPG) sheet is dry etched in oxygen plasma to many 5 μm deep mesa. The mesa was then stuck onto a photoresist and peeled off layers by a scotch tape (see Figure. 2.3). The thin flakes left on the photoresist were washed off in acetone and transferred to a silicon wafer. It was found that these thin flakes were composed of monolayer or a few layers of graphene. While, the mechanical exfoliation of graphene led to numerous exciting discoveries of graphene electronic and mechanical properties, such approach is limited by its low production.

Physical exfoliation approaches are desirable where it is required to maintain the graphene structure due to the structural defects. Graphite could be exfoliated in N-methyl-pyrrolidone to produce defect-free monolayer graphene. Such approach utilizes the similar surface energy of N-methyl-pyrrolidone and graphene that facilitates the exfoliation. However, the disadvantage of this process is the high cost of the solvent and the high boiling point of the solvent that makes the following graphene deposition difficult (Singh *et al.,* 2011).

Figure 2.3: Mechanical exfoliation of graphene using scotch tape from HOPG (Singh *et al.*, 2011).

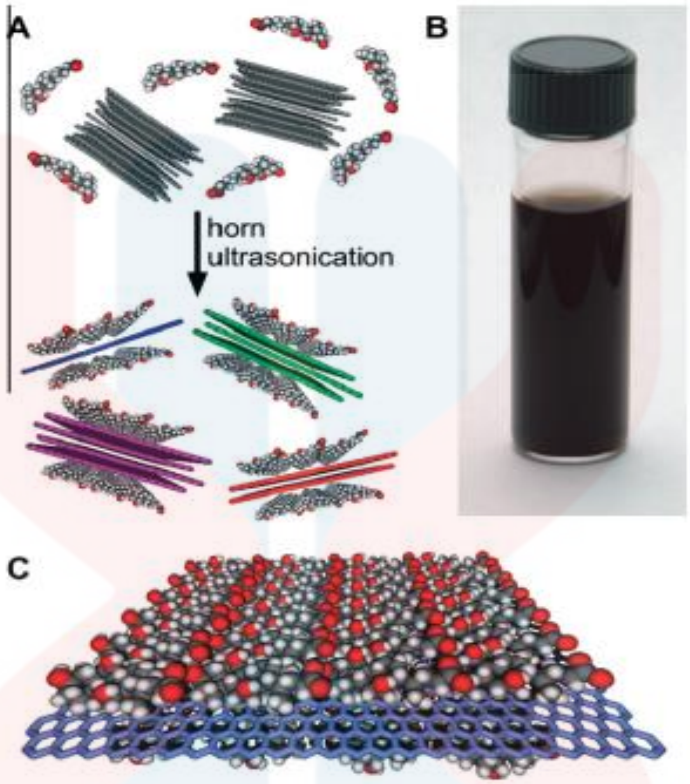

Figure 2.4: (A) Schematic illustration of the graphene exfoliation process. Graphite flakes are combined with sodium cholate (SC) in aqueous solution. Horn-ultrasonication exfoliates few-layer graphene flakes that are encapsulated by SC micelles. (B) Photograph of 90 lg mL1 graphene dispersion in SC 6 weeks after it was prepared. (C) Schematic illustrating an ordered SC monolayer on graphene (Singh *et al.*, 2011).

2.3 Chemically Derived Graphene

Chemically derived graphene holds great function as an electrode material owing to its unique physical and chemical properties.

2.3.1 Synthesis of Graphene Oxide and the Reduction

Low cost graphene can be produced in bulk through a chemical oxidation and reduction process using graphite as a raw material and the product obtained is known as reduced graphene oxide (RGO) (Sharmila *et al.,* 2015). Graphite oxide is commonly synthesized through the oxidation of graphite using oxidants including

concentrated sulphuric acid, nitric acid and potassium permanganate based on Hummers method (Singh *et al.,* 2011). The Hummers method uses a combination of $KMnO_4$ and H_2SO_4. Oxidation of graphite via this method can be done starting from various commercially available source, but graphite flakes is the most commonly used. However, this mechanism is very challenging to ascertain owing to the complexity of flake graphite and the inherent defects that may occur (Sundaram, 2014).

The reduction of GO using hydrazine vapour as a reductants, however require great care because it is both highly toxic and potentially explosive. Hydrazine hydrate, unlike other strong reductants, does not react with water and was found to be the best one in producing very thin and fine graphite-like sheets. During the reduction process, the brown colored dispersion of GO in water turned black and the reduced sheets aggregated and precipitated. RGO became less hydrophilic due to the removal of oxygen atoms and thus precipitated. The reason of re-establishment of the conjugated graphene network could be attributed to the reaction pathway (Singh *et al.,* 2011).

A number of several technique has been explored as an alternative tp hydrazine hydrate. For example, the use of sodium borohydride ($NaBH_4$), hydroquinone, gaseous hydrogen, vitamin C and strongly alkaline solution as a reductants. As an alternative to chemical method, there has been a research into method such as electrochemical reduction, photocatalytic reduction and reduction using photocatalytic flash (Sundaram, 2014). The morphology of RGO is characterized using scanning electron microscope (SEM). As shown in the Figure 2.6 fold structure is found on both the surface and the edge of RGO powder (Cao & Zhang, 2015).

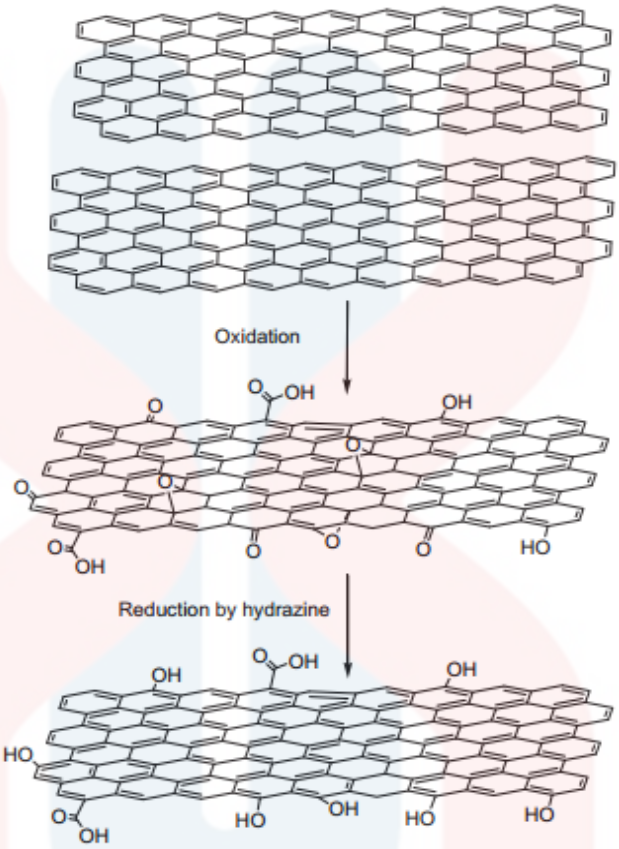

Figure 2.5: Oxidation of graphite to GO and reduction to RGO (Singh *e al.*, 2011).

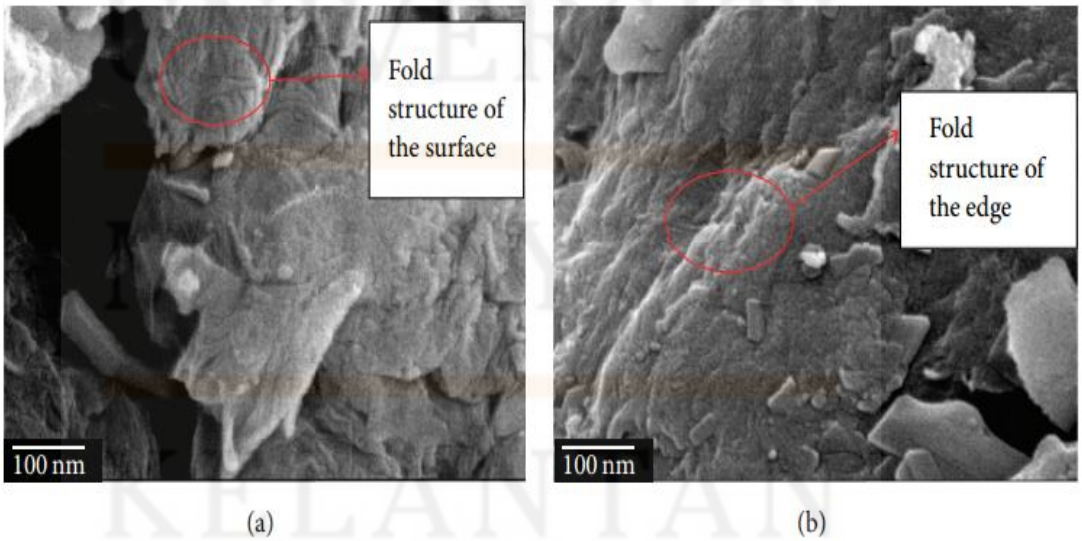

Figure 2.6: SEM morphology of RGO (Cao & Zhang, 2015).

2.3.2 Surface Functionalization of graphene oxide (GO)

The surface functionalization of GO is important in controlling exfoliation behaviour of GO and RGO (Singh *et al.,* 2011) An important step for more application of GO is further modifications of GO through covalent or non-covalent functionalization. Molecules, namely amines, can be fixed to the oxygenated functionalities on the surface or edge of GO sheets. Decorated GO, as a filler, can have chemical bonding with polymer chains, and are effective in improving the mechanical properties (Mallakpour *et al.,* 2015).

In covalent functionalization, oxygen functional groups on GO surfaces, including carboxylic acid groups at the edge and epoxy/hydroxyl groups on the basal plane can be utilized to change the surface functionality of GO. GO had been treated with organic isocyanates to give a number of chemically modified GO. Treatment of isocyanates reduced the hydrophilicity of graphene oxide by forming amide and carbamate esters from the carboxyl and hydroxyl groups of GO, respectively. Consequently, isocyanate modified graphene oxide readily formed stable dispersion in polar aprotic solvents giving completely exfoliated single graphene sheets with thickness of 1 nm. This dispersion also facilitated the intimate mixing of the graphene oxide sheets with matrix polymers, providing a novel synthesis route to make graphene–polymer nanocomposites. Modified GO in the suspension could be chemically reduced in presence of the host polymer to render electrical conductivity in the nanocomposites (Singh *et al.*, 2011).

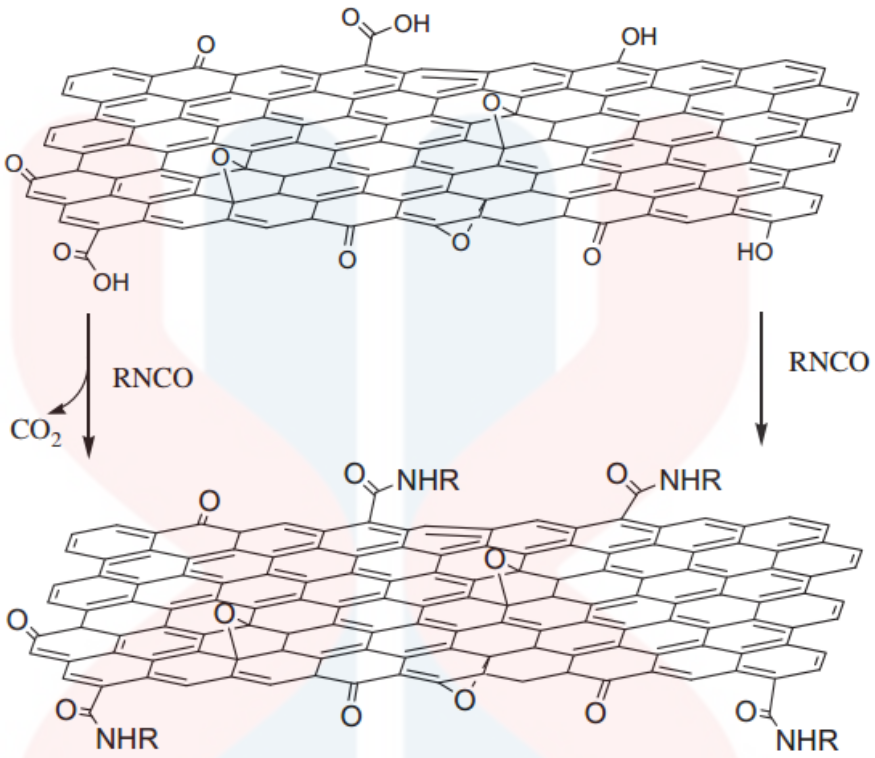

Figure 2.7: Isocyanate treatment of GO where organic isocyanate reacts with the hydroxyl and carboxyl groups of the GO sheets (Singh *et al.*, 2011).

The non-covalent functionalization of GO utilizes the weak interactions (i.e. π-π interaction, Van der Waals interactions and electrostatic interaction) between the GO and target molecules. The sp^2 network on GO provides p– p interactions with conjugated polymers and aromatic compounds that can stabilize RGO resulted from chemical reduction and produce functional composite materials. The conjugated polymers and aromatic compounds include poly(sodium4-styrenesulfonate) (PSS), sulfonated polyaniline, poly(3 hexylthiophene) (P3HT), conjugatedpolyelectrolyte, 7,7,8,8 tetracyanoquinodimethane anion, tetrasulfonate salt of copper phthalocyanine (TSCuPc), porphyrin, pyrene and perylenediimide decorated with water-soluble moieties, and cellulose derivatives.

During the chemical reduction of GO, RGO nanosheets are stabilized via the interaction between aromatic molecules and reduced graphene oxide nanosheets. Aromatic molecules have large aromatic plane and can anchor onto the RGO surface without disturbing its electronic conjugation, providing stability for reduced graphene oxide (Singh *et al.*, 2011). For example, RGO sheets have been modified by polyindole (Pin) via in-situ chemical oxidation method to obtain stable dispersion in water and incorporation of Ag nanoparticles (AgNPs), resulting in Ag-RGO nanocomposite for electrochemical applications (Dubey *et al.*, 2015).

2.4 Properties and Applications of GO and RGO

Several approaches have been demonstrated in this regard which involve drop cast, dip coating, spraying, spin coating, Langmuir–Blodgett (LB) film, and vacuum filtrations deposition. The GO and RGO can be deposited either on prefabricated electrode patterns or the electrodes can be defined after deposition of GO and RGO. Using these processes, the devices using single layer, few layers and thin film have been fabricated. For single layer and few layer devices, the throughput can be low since the processes involve random placement of GO and RGO sheets. Thin film deposition can improve the throughput. The drop cast, dip coating, and spray depositions on the substrate are convenient ways to build GO and RGO devices. The advantages of these techniques is non-uniform film thickness on substrate, due to aggregation of GO/RGO sheets. In spin coating, the thickness of layer can be tuned by varying the concentration of the graphene dispersion. Suspension of GO in a mixture of water and methanol carefully spreads over the water surface to obtain the floating GO sheets trapped at the water or air interface. The floating GO film is then deposited onto a substrate as it is slowly raised from the solution. This process can be repeated to make layer by layer deposition of RGO film of desired thickness. The

filtration technique involves filtration of the suspension containing the GO sheets through porous membrane. The as-filtered GO sheets are then transferred from the filter membrane to the substrate surface. The thickness of each GO paper sample can be controlled by adjusting the volume of the colloidal GO suspension. All of these technique can provide a convenient route to produce large quantity RGO thin film devices (Singh *et al.,* 2011).

2.5 Defect Density in Chemically Derived Graphene

There are two kinds of defects in graphene. One is point defects, typically vacancies or interstitial atoms are zero-dimensional. The other is on one dimensional line of defects. The defects are not always stationary and that their migration can have an important influence on the properties of a defective crystal. In graphene, each defect has certain mobility parallel to the graphene plane. The mobility might be immeasurably low, for example, for extended vacancy complexes, or very high, for example, for diatoms on an unperturbed graphene lattice. The migration is usually governed by an activation barrier which depends on the defect type and therefore increases exponentially with temperature (Liu *et al.*, 2015).

2.5.1 Stone-Wales Defect

The Stone–Wales (SW) defects are one typical defect in the carbon nanostructures. There are two distinct orientations of SW defects namely type I, and type II, which caused by 901 rotation of c–c bond in different directions (Ebrahimi, 2015). It has the lowest transformation energy among all intrinsic defects in graphenic systems, but also is shown to be energetically more favorable than in carbon nanotubes (CNTs) or fullerenes (Zhao *et al.,* 2015).

2.5.2 Single Vacancies

Single atom defects in graphene lead to the occurrence of quasi-localized states near the Fermi level (Scopel *et al.,* 2016). Single vacancies (SV) in graphene has experimentally observed by Transmission Electron Microscopy (TEM). The SV undergoes a Jahn–Teller distortion which leads to the saturation of two of the three dangling bonds toward the missing atom. One dangling bond always remains owing to geometrical reasons. This leads to the formation of a five-membered and a nine-membered ring (Liu *et al.,* 2015).

2.5.3 Multiple Vacancies

Double vacancies (DV) can be created either by the coalescence of two SVs or by removing two neigbouring atoms. Because no dangling bond is present in a fully reconstructed DV, two pentagons and one octagon appear instead of four hexagons in perfect graphene (Liu *et al.,* 2015).

2.5.4 One Dimensional Defects

This kind of defect has been observed in many experimental studies of graphene. These line defects are tilt boundaries separating two domains of different lattice orientations with the tilt axis normal to the plane. Such defects can be thought of as a line of reconstructed point defects with or without dangling bonds. One example is a domain boundary which has been observed to appear due to lattice mismatch in graphene grown on a Ni surface (Liu *et al.,* 2015).

2.5.5 Defects at the Edges of Graphene

Each graphene layer is terminated by edges with the edge atom being either free or passivated with hydrogen atoms. Armchair and the zigzag orientation are the

simplest edges structures. Defective edges can appear because of local changes in the reconstruction type or because of sustained removal of carbon atoms from the edges. This can be achieved by sputtering edge atoms. Under these conditions, armchair edges can be turned to zigzag edges. An intermediate structure can be regarded as a defective edge. A simple example of an edge defect is the removal of one carbon atom from a zigzag edge.

2.6 Application of RGO

RGO can be used in various field of aaplication, including sensors and biosensors, as Quantum blackode array, solar cell, phototransmitter, photodetector and also as transparent electrode.

2.6.1 Sensors and biosensors

Graphene and graphene-related materials have been used to fabricate biosensors for the detection of a number of clinically relevant biomarkers, including glucose, bacteria, DNA, and biomarkers relevant to cancer (Guy & Walker, 2016). Graphene could be an excellent electrode material for oxidase biosensors (Shao *et al.,* 2010). In sensing applications graphene has been used as RGO, a layered material produced by the oxidation of graphite. RGO is strongly oxygenated, bears functional groups on the hydroxyl and epoxy basal planes, in addition to carbonyl groups and carboxyl groups located on the edges of the floors. The presence of these functional groups makes RGO strongly hydrophilic and therefore readily dispersible in water thus facilitating the drop casting procedures used for the modification of electrode surfaces. RGO is a poor conductor, but the treatment with heat, or by chemical reduction, it restores most of the properties of the original graphite. There are 19 different electrochemical sensors and biosensors based on nanoparticle-decorated and doped 2D-graphene for enzymatic and non-enzymatic detection of

different biomarkers employed for different types of diseases (Bollella *et al.,* 2016). For gas sensors, Graphene exhibits a properties that make it an ideal candidate for the ultrahigh sensitivity detection of different gases existing in various environments (Yavari & Koratkar, 2012).

Each electrode modification is based on different methods to synthesize the graphene, making sometimes difficult the direct and rigorous comparison about the performances of the various however related sensors. The division of electrochemical sensors and biosensors into three classes which is for glucose, for hydrogen peroxide and for other biomarkers was requested due to the extraordinary large number of papers regarding glucose detection, the most important human biomarker, and hydrogen peroxide, an essential compound involved in many biological processes, compared to other biomarkers (Bollella *et al.*, 2016).

Besides that, RGO sheets decorated with Fe_2O_3 nanoparticles exhibited exceptional performance in energy storage and conversion, especially as anode materials for lithium ion batteries as well as for catalysis and magnetic recording, as gas sensors and in water treatment (Sharmila *et al.,* 2015). For biological applications of GO/RGO, RGO-based single-bacterium biodevice, label-free DNA sensor, bacterial DNA or protein and polyelectrolyte chemical transistor have been reported. GO sheets are biocompatible without obvious toxicity and employed GO for drug delivery (Zhuang Liu *et al.,* 2009). GO has distinct advantages in biological applications over other related materials such as carbon nanotubes (CNTs) and fullerene. First, it has excellent water solubility without the cutting and de-bundling process required for CNTs. Second, it does not have the oxidative stress originating from metallic catalyst impurities, the latter being a cause of CNT-induced toxicity. Third, it does not require surfactants for dispersion; some of the observed

cytotoxicity in CNT has been linked to surfactants. Lastly, it has high specific surface area, which allows for the high-density loading of drugs through electrostatic bonding (Loh *et al.,* 2010).

2.6.2 RGO as Graphene Quantum Dot Array: Coulomb blockade effect

RGO can be modeled as a two-dimensional array of graphene quantum dots (GQD), where graphitic domains act like quantum dots while oxidized domain behave like tunnel barriers. This has been verified in the low temperature electrical conduction in in few layers RGO (Singh *et al.,* 2011). GQD are a type of zero dimensional graphene with lateral dimensions of less than 100 nm, and they have received enormous attention due to their unique chemical, electronic and optical properties from quantum confinement and edge effects (Tam *et al.,* 2015) GQD have been synthesized, leading to novel applications in photodetection, photovoltaics, light-emitting diodes (LEDs), and plasmonics. The difference between graphene quantum structures and graphene is the modification of electron behavior due to quantum confinement. When graphene is reduced to a size comparable to the exciton Bhor radius, quantum confinement effects become observable. In addition, the particular size, shape and edge structure all affect the electrical and optical properties of any particular graphene quantum structure (Jin *et al.,* 2015).

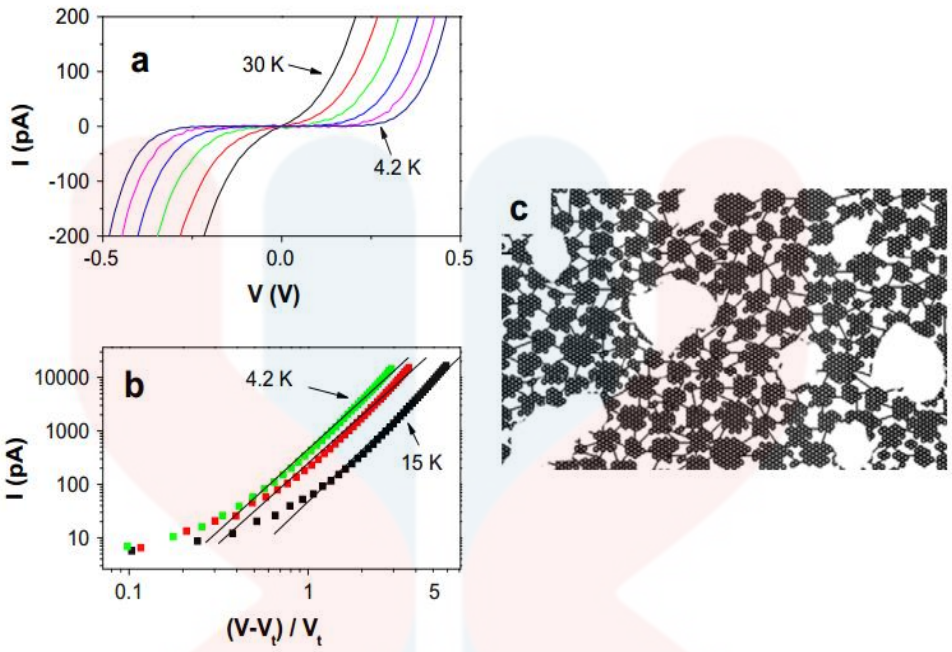

Figure 2.8: (a) Current(I)–voltage(V) characteristics of a representative RGO device at temperatures 30, 25, 20, 15, 10 and 4.2 K. Below 15 K, the current is zero for V < due to coulomb blockade of charges. (b) I vs. (V -)/ t curves plotted in a log–log scale. Slope of the curves gives the value of exponent a = 3.1, 3.3, and 3.4 at 4.2 K, 10 K, and 15 K respectively. (c) Schematic of RGO as GQD array. The light gray areas represent GQDs, the white regions represent oxidized carbon groups and topological defects. The lines between GQDs represent tunnel barriers (Singh *et al.*, 2011).

2.6.3 RGO as Solar Cell

One uses single-layer graphene as the charge carrier, while the other employs a graphene thin film as a transparent electrode for dye sensitized solar cells and organic photovoltaic devices. Both kinds of solar cell have shown good performance, which stimulates us to develop an inorganic–organic hybrid solar cell with graphene as a transparent electrode (Yin *et al.*, 2010). RGO transparent electrodes can be used for solar cell electrode. Several studies suggest that GO and RGO can also be used as hole transport layer as well as a part of active material (Singh *et al.*, 2011). For example, the reduction of GO at room temperature with Vitamin C for RGO-TiO_2 photoanode in dye-sensitived solar cell. DSSCs are comprised of photoanode (the

most frequently used material is anatase TiO_2) decorated by a monolayer of dye molecules (sensitizers), a platinized counter electrode, and an electrolyte solution with a dissolved iodide ion/tri-iodide ion redox couple at the electrodes. The transport progress of photogenerated electrons across the TiO_2 nanoparticle network becomes the major bottleneck of improving the conversion efficiency of DSSCs. If the photogenerated electrons do not accomplish the transportation, they will recombine with the holes and get annihilated in the TiO_2 nanoparticle network. To enhance electron transfer ability and suppress the recombination, some charge carriers materials are introduced into photoanode to the direct photo electrons. The average conductivity of the RGO reduced with VC is comparable with that reduced using hydrazine or hydrothermal method (Ding *et al.*, 2015).

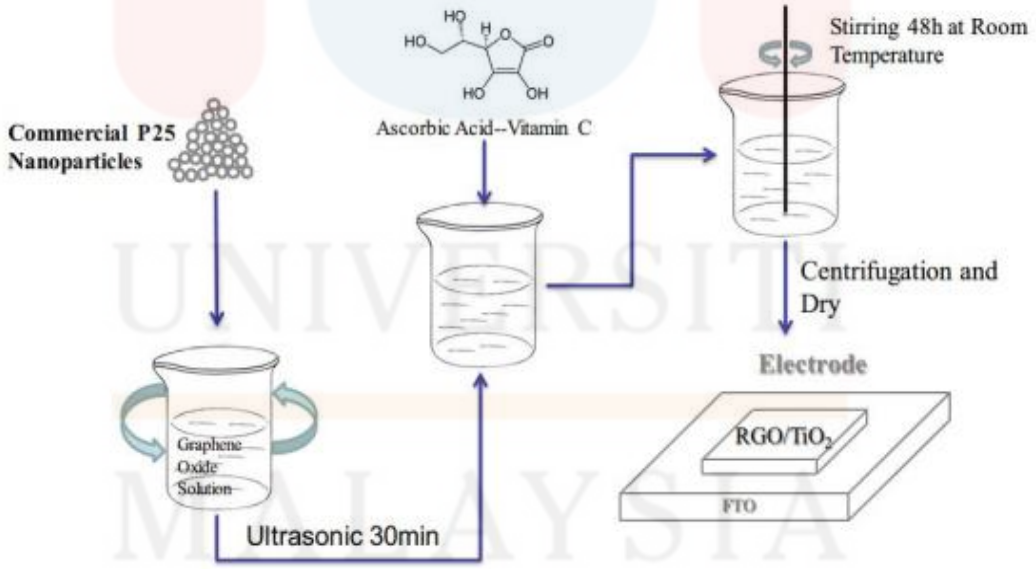

Figure 2.9: Fabrication process for RGO-Ti photoanodes (Ding *et al., 2*015).

2.6.4 Graphene Film as Transparent Electrode

It has been demonstrated that thin film (<30 nm) of RGO is semi-transparent to visible and NIR region while thick films are opaque. The transmittance and

conductivity of the GO/RGO film can be tuned by tuning the thickness of the film and the degree of reduction. The transparency of RGO varies with film thickness *(Singh et al.,* 2011).

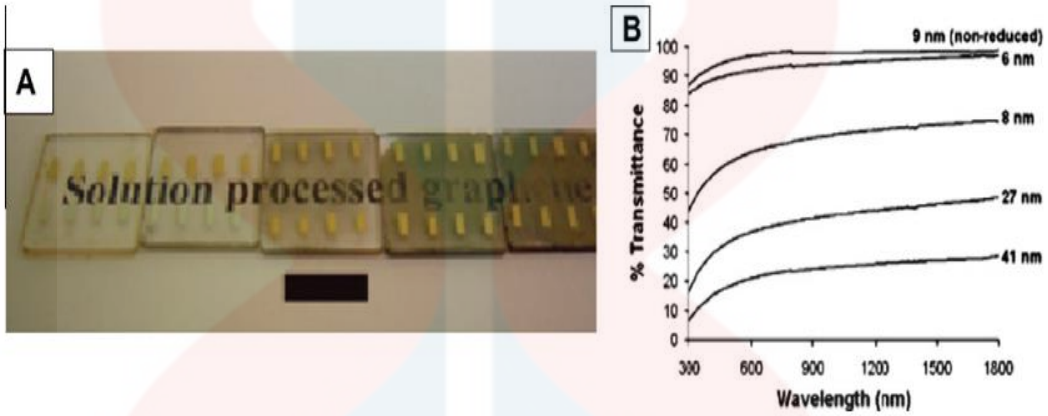

Figure 2.10: Optical and electrical characterization of spin coated GO films on quartz. (A)Photograph of an unreduced (leftmost) and a series of high-temperature reduced GO films of increasing thickness. Black scale bar is 1 cm. (B) Optical transmittance spectra of the films in (A) with the film thickness indicated.

As the film gets thicker, the transmittance will reduced. The relationship can be seen when the conductivity of the RGO thin film increases with the degree of reduction, transmittance will decrease (see Figure 2.10). Therefore, the optimization of film thickness and reduction parameters is important to obtained high performance transparent and conducting RGO thin film. Due to their conducting, transparency and flexible nature, RGO thin film is considered to be a good electrode material for organic electronic and optoelectronic application. RGO electrodes has several advantages including, water soluble properties, the homogeneity and composition of the films are simply determined by the composition of the parent suspension and surface modification of the substrate, relatively inexpensive starting materials, and low temperature and high throughput processing (Singh *et al.*, 2011).

2.6.5 RGO for Photodetector, Phototransistor and Emitter

Photoconductivity of bulk RGO thin film has been studied using various intensities of light, external field, and photon energies. The study showed higher photocurrent under same photon energy with the increase of incident light intensity and external electric field. This shows that the charge carrier generation is influenced by the number of photons and the external field intensity in RGO sheets. Higher photoconductivity has also has been observed with higher photon energy under same condition. It can be concluded that the RGO film generates more charge carriers per unit volume upon irradiation of higher photon energy. RGO film shows high photocurrent generation efficiency, compared to the SWNT.

RGO FET phototransistor also has been studied based on their energy band gap values. In this study, RGO FET, in which few layer RGO sheets serves as the semiconducting channel and is designed to conduct positive and negative charge carriers respectively (Singh *et al.*, 2011).

2.6.6 GO-Ag as Optical Sensor for the Detection of ion

Silver forms amalgam with Hg and the redox potentials are appropriate for galvanic replacement reaction with Hg^{2+} ion adsorption of mercury ions, redox reaction with them, as well as amalgamation can sensitively influence the surface plasmon resonance (SPR) extinction of Ag nanoparticles, the latter provides a relatively cheap (compared to Au nanoparticle based sensors) and efficient (as the molar extinction coefficients are much higher than that of Au nanoparticles, route to monitor mercury in all its oxidation states. The advantages of Ag compared to Au is higher sensitivity to oxidation and greater susceptibility to degradation during functionalization (Ramesh & Radhakrishnan, 2011).

However, in the case of bare Ag NPs, a strong interparticle coupling effect may reduce the interaction of Hg^{2+} and consequently affects the detection response. It is known that the Ag NPs display a SPR absorption band at around the wavelength of 420 nm and it is very sensitive to the analytes (Noor *et al.,* 2015).

Silver nanoparticles (AgNPs) attracted much attention due to its high catalytic activity, electronic and optical properties. The AgNPs possess a principal absorption band in the region of 400 nm due to the localized surface plasmon resonance (LSPR). Among the investigated analytes, heavy metal ions especially Hg^{2+} ions are more often monitored with AgNPs through the optical sensing method because of its high toxicity and solubility in water. Mercuric (Hg^{2+}) ions are mainly released into the atmosphere from solid waste incineration, power plants, and burning fossil fuels that pollute water, soil and air. The existence of Hg^{2+} ions in water causes serious damage to the brain, nervous system, kidneys and endocrine system of living organisms. Developing a system for detecting with high sensitivity and selectivity against other common metal ions dissolved in water is a challenge in recent years. From an environmental point of view the development of an inexpensive, simple, selective and sensitive method of detection Hg^{2+} ions of becomes highly important (Kamali *et al.,* 2015).

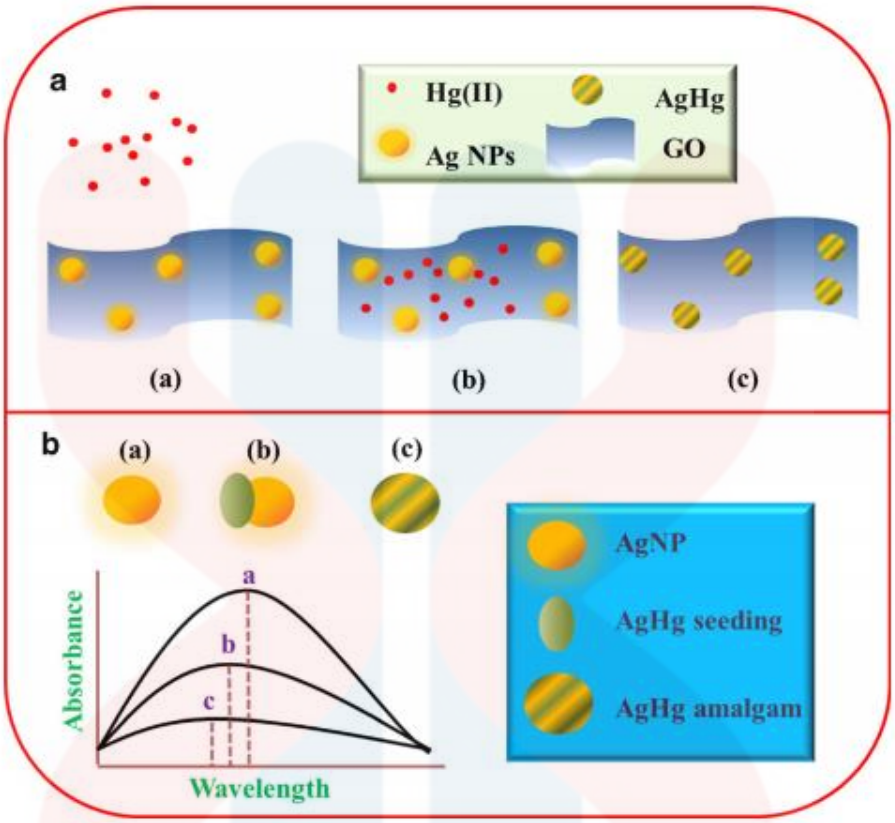

Figure 2.11: A Schematic explaination the function of GO in the detection Hg^{2+} ions. (a) Addition of Hg^{2+} ions into a solution containing Ag/GO nanocomposite. (b) Adsorption of Hg^{2+}ions on the surface of GO. (c) Interaction of Hg^{2+} ions with Ag NPs and formation of AgHg amalgam. b Schematic representation of the formation of AgHg amalgam and its influence in absorption spectra of the Ag NPs present in the Ag/GO nanocomposite (Kamali *et al.*, 2015).

CHAPTER 3

MATERIALS AND METHODS

3.1 Materials

The materials that has been used in this experiment are 3 g of graphite powder, 18 g of potassium permanganate ($KMnO_4$, 320 mL of sulphuric acid (H_2SO_4), 80 mL of phosphoric acid (H_3PO_4), 7 mL hydrogen peroxide (H_2O_2), 500 mL ice, 50 mL of 1 M hydrochloric acid (HCI), 10mL of 10 μL ammonia, NH_3 (25%) with 10 mL of silver nitrate, (10 mM $AgNO_3$, 10 mL $AgNO_3$ (10 mM) and mercuric chloride ($HgCl_2$).

3.2 Method

The method include the preparation of GO using Simplified Hummer's method and synthesizing GO-Ag nanocomposite using microwave irradiation for 60 seconds.

3.2.1 Preparation of GO

Graphene oxide (GO) was prepared from natural graphite using simplified Hummer's method. About 3 g of graphite flakes was mixed with 320 ml of H_2SO_4, 80 ml of H_3PO_4 and 18 g of $KMnO_4$ to produce mixture A. Mixture A was stirred for 3 days to achieve maximum oxidation of graphite (Noor *et al.*, 2015).

Figure 3.1: Mixture A was stirred for 3 days on a hot plate.

After the color changed from dark purplish green to dark brown, H_2O_2 was added to stop the oxidation of graphite. The highly oxidation level of graphite can be monitored by the bright yellow color of the solution. 500 ml of ice is added to the mixture to slow down the exothermic reaction (Noor *et al.*, 2015).

Figure 3.2: Mixture A was added to the 7 ml of H_2O_2 in 500 ml ice.

The solid GO obtained were washed with 1M of HCl for 3 times, followed by deionised water for 7 times until pH 5 was obtained. This step is crucial to make sure the excess metal ions was removed. The centrifugation of GO took place at 10000 rpm at 20ºC by using High Speed Centrifuge Supra 22K (Noor *et al.*, 2015).

Figure 3.3: High Speed Centrifuge Supra 22K.

Figure 3.4: GO were put in the centrifuge tube. The mixture were equally divide into 6 centrifuge bottles. The mass of the mixture were ensure to be balanced before the centrifuge were run.

Figure 3.5: GO mixture after being washed for 4 times.

Figure 3.6: GO Gel were obtained after being dried under vacuum.

3.2.2 Synthesizing of GO-Ag Nanocomposite

GO-Ag nanocomposite were synthesized using silver-ammonia complex solution that was prepared by adding 100 µL of ammonia (25 wt.%) slowly into 10 ml of 10 mM $AgNO_3$ solution and the mixture was vigorously stirred. Then, the stirred solution were mixed with 1 mL of aqueous GO solution (0.1 mg/mL) and the mixture were sonicated for 5 min using Ultrasonic bath. A yellowish brown color solution of GO-Ag nanocomposite were obtained and the product were centrifuged with a centrifugation force of 10,000 g, washed with deionized water for three times. For the optimization of the synthesis, the nanocomposite was prepared with lower concentration of ammonia solution. Then, the GO-Ag nanocomposite solution were undergo microwave irradiation for 60s and allowed to cool at room temperature. Microwave irradiation act as external source that facilitate the attachment of Ag NPs on GO surface.

Figure 3.7: Microwave for synthesising GO-Ag.

3.3 Characterization of GO and GO-Ag

The GO that has been produced were analysed by using several technique including X-Ray Diffraction (XRD), Fourier Transform Infrared Spectroscopy (FTIR), and Transmission Electron Microscopy (TEM). The element analysis will be determined using XRD and the infrared spectrum of absorption or emission of GO will be determine using FTIR. The morphology of the nanocomposite and size of the Ag NPs were examined by the transmission electron microscopic (TEM) instrument (Philips CM12) operated at 200 kV. All the technique will help to identify the characteristics and properties of GO and at the same time it can be determine the percentage of the material content in the product produced.

3.4 Optical detection of Hg^{2+} ion

The optical sensing of GO-Ag will be performed using Thermo Scientific Evolution 300 UV-vis spectrophotometer. The best analytical wavelength for analyzing ions is found to be 420 nm.

For optical detection, a specific concentration of the metal ion solution was added into 2 mL of GO-Ag solution, shaken well and subjected to a constant resting

time (1 min) before the color changed was observed. 200 µl of Mercuric ion, Hg^{2+}, lead (II) nitrate, nickel (II) chloride and zinc sulphate solution were used. The best analytical wavelength for analyzing ions is found to be 420 nm.

CHAPTER 4

RESULTS AND DISCUSSION

4.0 Introduction

This chapter discusses all the results and analyse from the experiments. The results have been gained through the experiment. Parametric studies on various concentration of silver complex in graphene oxide solution. Graphene oxide was used because it can easily mixed with Ag salt to obtain a scalable quantity of nanocomposites via a chemical reduction. Mercury (Hg) is a toxic material that exist in metallic, inorganic and organic forms. Due to the harmful effects of Hg^{2+}, it is crucial to be able to detect and measure the level of Hg^{2+}. Ag NPs based optical assays have been successfully used in the detection of Hg^{2+} in aqueous medium in a simple and effective method (Noor *et al.*, 2015).

This research was aim to study the synthesis of silver-graphene oxide using a microwave and its application for the determination of mercury ion, Hg^{2+}. Experimental method was design as discussed in Chapter 3. Data is discussed in the forms of figures and graphs.

4.1 Choice of materials

The GO-Ag nanocomposite were chosen as an assay for optical determination of Hg^{2+}. GO serve as an effective host material for the growth of Ag NPs due to the presence of surface functional groups and high specific surface area. The functional group present in the GO can prevent the agglomeration of Ag NPs, thus the surface area of a Ag nanoparticles can be fully available for the interaction of Hg(II). Ag NP

display a SPR absorption band at around the wavelength of 420 nm and it is very sensitive to analytes. The position of the SPR band depends on the Ag NP size and the local environment. The Ag NPs based assay is highly preferred for the determination of Hg^{2+} due to its low cost when compared to the other noble metal nanoparticles such as gold, platinum or palladium (Noor *et al.*, 2015).

4.2 XRD Analysis

X-ray diffraction (XRD) was used to identify the characteristic of GO and GO-Ag peak. The information gathered from the peak was used to determine the presence of Ag NPs on the graphene sheets.

4.2.1 Phase Identification

Structural analysis of GO-Ag nanocomposites was carried out by X-ray diffraction (XRD) study (see Figure 4.3). From the XRD pattern, it can be seen that the characteristic GO peak centered at 10.0º corresponds to the (0 0 1) reflection of GO due to its crystalline nature (Sahu *et al.*, 2015). After 60 seconds of microwave irradiation on the GO-Ag nanocomposite, the peak at 10º shifted to 13º and a broad peak appeared at around 20º which suggests the reduction of the GO. At this state, GO was not fully reduced to the RGO after 60 seconds of microwave irradiation. Therefore, the functionalization of the GO surface with the Ag may prevent the graphene sheets from restacking. The formation of AgNP was confirmed by the existence of diffraction pattern of silver crystal structure. The diffraction peaks for the sample GO at 30º, 40º, 45° and 68° correspond to the face centre cubic (fcc) of Ag at (1 1 1), (2 0 0), (2 2 0) and (3 1 1) with (JCPDS card no. 89-3722). These have further confirmed the formation of Ag crystals in both samples by using microwave irradiation method. The simultaneous presence of the characteristic peaks of GO and

Ag NPs, in the nanocomposite gives the evidence regarding the formation of silver nanoparticles imprint graphene nanosheets (Sahu *et al.*, 2015).

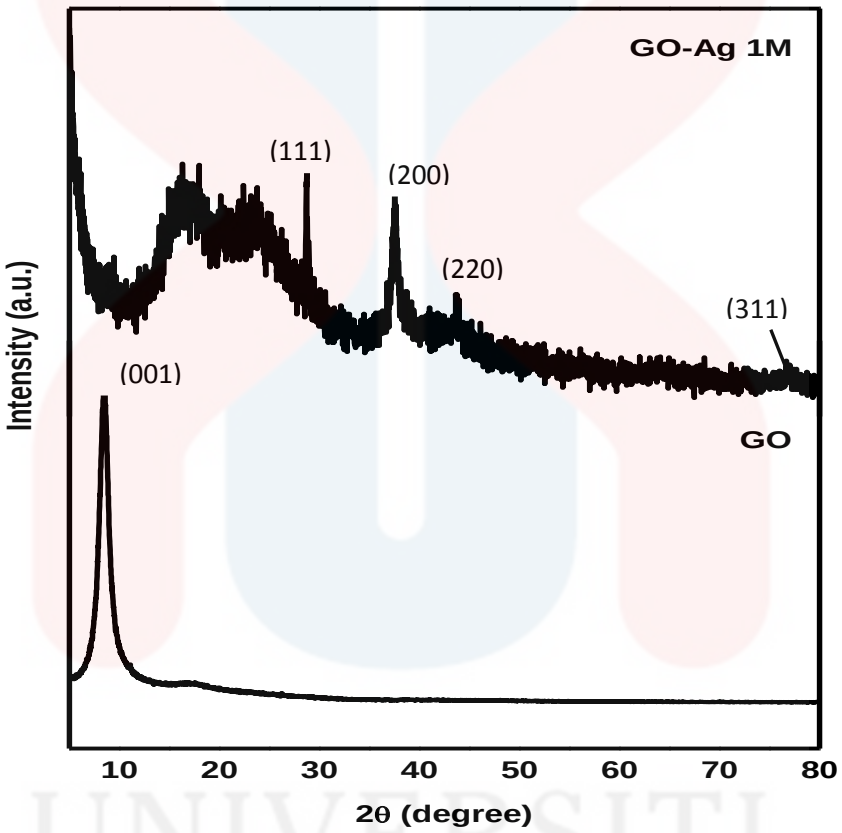

Figure 4.1: XRD pattern on GO and GO-Ag.

4.3 FTIR Analysis

The result obtained from the FTIR (see Figure 4.4) suggested that the GO was partially reduced during the synthesis of GO-Ag. Therefore, the disrupted conductivity of GO might be restored during the reduction process and subsequently enhance the electron movement from Ag within the GO sheets. There is a significant decrease in the intensity of the adsorption bands of the oxygenated functional groups

for the GO-Ag sample. This can be due probably to the existence of Ag NP on the surface of GO and also to the slight reduction of GO by microwave during the synthesis of the GO-Ag nanocomposite. In the case of GO, the broad and intense peak centered at 3040 cm^{-1}, which is related to OH groups and the strong peak at 1620 cm^{-1} corresponds to the stretching vibrations of of C=O carboxylic moieties. The peak at 1420 cm^{-1} is associated with the skeletal vibrations of aromatic C=C bond, or intramolecular hydrogen bonds. Peak at 1049 cm^{-1} correspond to C-O-H deformation. Therefore, it confirms the existences of the abundance of hydroxyl groups and oxygenous groups on the surface of GO, which makes GO to be convenient for further modification with plasmonic NPs, namely Ag NPs.

For GO-Ag nanocomposite, the graph is slightly constant at 3040 cm^{-1}. This is due to the silver nanoparticles that embedded to the surface of GO, which makes GO less visible. The intensity of C=O carbonyl stretching at 2328 cm^{-1} decreased, whereas, the aromatic C=C vibrations at 2100 cm^{-1} of GO nanosheets increased. This change can prove that there is an interaction between AgNPs and the oxygen-containing functional groups (i.e., −COOH) of GO nanosheets by forming a chemical bond or electrostatic attraction.

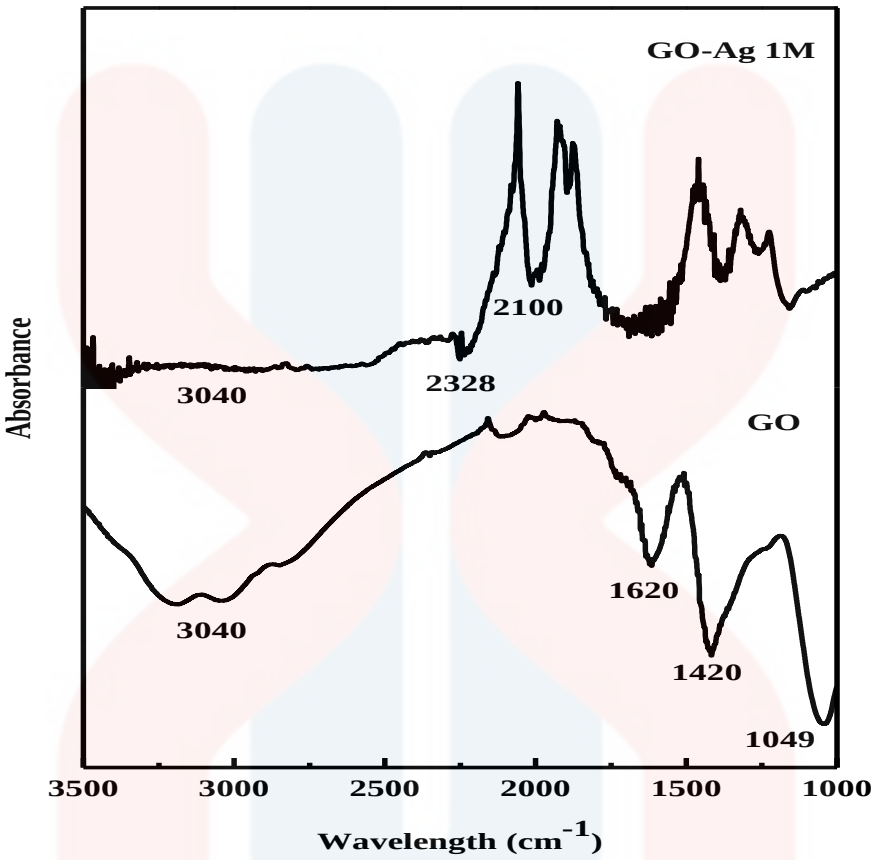

Figure 4.2: FTIR spectra of GO and GO-Ag.

4.4 Optical properties

The optical of GO-Ag is determine using colorimetric detection of GO-Ag with Hg^{2+} and several metal ions. The reaction of GO-Ag with these metal ions were recorded to determine the optical properties of GO-Ag. Uv-vis spectra analysis were carried out to determine the suitable visible wavelength of GO-Ag for the determination of Hg^{2+}.

4.4.1 Optical determination of Hg^{2+} ion

For colorimetric detection, an optimum concentration level of different metal ions were added separately into the GO-Ag nanocomposite solution, shaken well,

and allowed to rest and the color changes were observed with bare eyes. The color change of GO-Ag nanocomposite solution were observed after individual addition of 200µl of Hg^{2+} ion (see Figure 4.5) and 200µl of other environmentally relevant metal ions such as lead(II) nitrate, nickel (II) chloride and zinc sulphate (see Figure 4.6). It was noticed that only with the addition of Hg^{2+}, GO-Ag nanocomposite solution will turned colorless, whereas the nanocomposite solution will remained the same after the addition of 200µl of other metal ions.

This results concluded that the GO-Ag nanocomposite is highly selective toward the determination of Hg^{2+} in the presence of other common toxic metal ions. The functional groups present in the GO prevented the agglomeration / aggregation of Ag NPs and hence, the surface area of Ag NPs could be fully available for the interaction of mercuric ions.

Figure 4.3: GO-Ag before and after addition of 100µl and 200µl of Hg^{2+} ion.

Before	After
 GO-Ag	 GO + Pb^{2+}
 GO-Ag	 GO + Ni^{2+}
 GO-Ag	 GO + Zn^{+}

Figure 4.4: GO-Ag before addition (a, c and d) and after addition (b,d and f) of Pb^{2+} Ni^{2+} and Zn^{+}.

4.4.2 UV-vis spectra analysis

The UV-vis spectra of GO and GO-Ag are shown in Figure 4.6. The GO sample shows a strong absorption peak at 230 nm which is due to the $\pi \longrightarrow \pi^*$ transitions of aromatic C-C bonds, and a shoulder peak at ~300 nm corresponds to n-

π* transitions of C=O groups present in GO. After microwave irradiation on the mixture GO-Ag, a new peak appeared 420 nm indicating the the formation surface plasmon resonance (SPR) absorption band of the Ag NPs. This phenomenon happened when the incident light interacted with the valence electrons at the outer band of AgNP leading to the oscillation of electron along with the frequency of the electromagnetic source.

There is a broad absorption range for the AgGO sample at 210 to 240 nm, which can be attributed to the presence of GO.The appearance absorption peaks at 227 nm and 300 nm remain with less intensity after the formation GO-Ag nanocomposite and it suggests that the partial reduction of GO might occur during microwave synthesis.

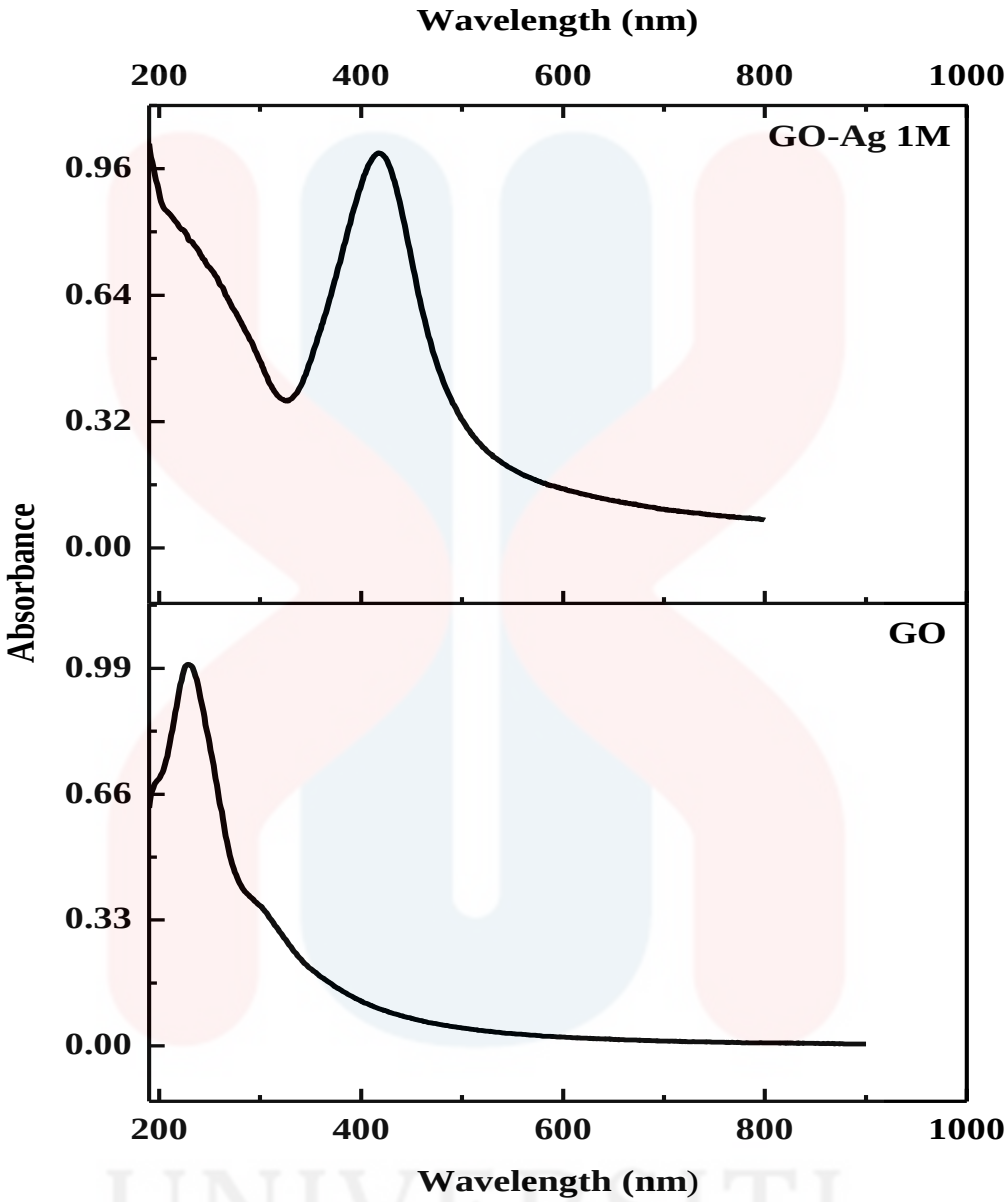

Figure 4.5: UV-vis spectra analysis of GO and GO-Ag.

4.5 Morphology of GO and GO-Ag nanocomposite

TEM analysis was performed to study the morphology of the GO-Ag nanocomposite. Figure 4.7 displays the TEM displays the TEM images with 200 nm magnification recorded for GO-Ag nanocomposite. It can be seen that the successful deposition of poly-dispersed spherical Ag NPs on GO sheets. The spherical shape of AgNPs relies on the single SPR absorption feature. AgNPs were deposited randomly

on the GO sheets. The deposition of AgNP on the upper and bottom layers of the translucent GO sheets can be differentiated by the black-and white contrast of the particles. These results suggest that GO sheets play an important role in the process of nucleation and stabilization, allowing the formation of smaller nanoparticles. Another observation is that GO appears to act as a morphological driver or controller for silver nanoparticles, dictating the formation of spherical-like particles in the GO-Ag nanocomposite (Moraes *et al.*, 2016).

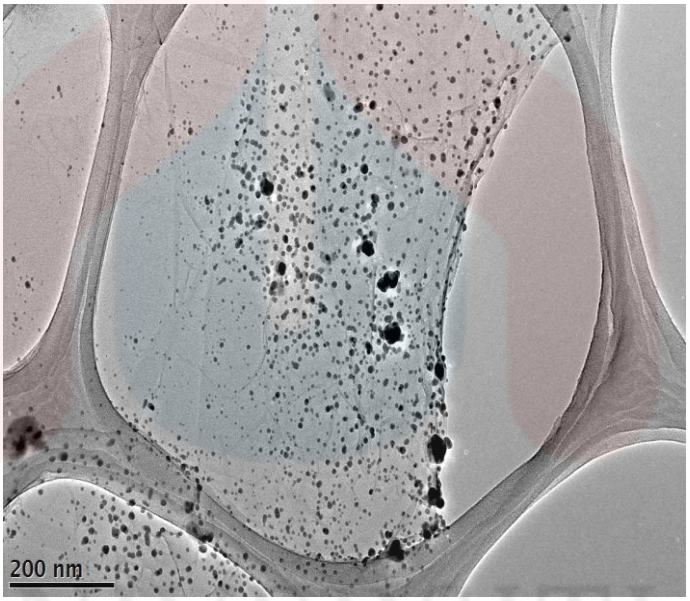

Figure 4.6: TEM image of GO-Ag with 200 nm magnification.

CHAPTER 5

CONCLUSION

5.0 Project Overview

The final part of the thesis gives an overview of the work and achievement of the project. A review of the results gained, through experimental method as well as project achievement has been presented. Finally, the recommendation of the projects are discussed for future work direction

5.1 Conclusion

From the results above, it can be concluded that GO were successfully synthesized using Simplified Hummer's method, in which this method replaced the use of hydrazine which is high in toxicity, with potassium permangate. It also can be concluded that GO-Ag nanocomposite were successfully synthesized using microwave irradiation method. Microwave irradiation method provides a rapid and green method for the synthesis of GO-Ag. It favors the formation of small and uniform nanoparticles through a fast and homogenous nucleation and crystallization. The nanocomposite was successfully characterized by XRD, FTIR, UV-visible absorption spectra and TEM. During the optical determination of Hg^{2+}, the change in color of GO-Ag nanocomposite were observed. The nanocomposite exhibited an excellent selectivity toward the determination of Hg^{2+} ion compared to the other metals ions.

5.2 Suggestions for future work

Several suggestions have been made to improve the method of synthesising GO. Currently, Hummer's method which use $KMnO_4$, $NaNO_3$ and H_2SO_4 is the most common method used most preparing graphene oxide. By increasing the amount of $KMnO_4$, the efficiency of oxidation process can be increased. This improved method provides a greater amount of hydrophilic oxidise graphene material as compared to Hummer's method.

In this experiment, microwave irradiation were done for 60 seconds to reduce the GO. Microwave irradiation time could be increase up to 2 or 3 minutes to fully reduce the GO to become reduced graphene oxide (RGO). Besides that, other reducing agents such as glucose, vitamin C or hydroquinone could be used to facilitate the reduction of graphene oxide within a short time.

References

Avouris, P., & Dimitrakopoulos, C. (2012). Graphene : synthesis and Graphene , since the demonstration of its easy isolation by the exfoliation of. *Materials Today*, *15*(3), 86–97.

Bollella, P., Fusco, G., Tortolini, C., Sanzò, G., Favero, G., & Gorton, L. (2016). Beyond graphene electrochemical sensors and biosensors for biomarkers detection. *Biosensors and Bioelectronic*, 4–5.

Cao, N., & Zhang, Y. (2015). Study of Reduced Graphene Oxide Preparation by Hummers ' Method and Related Characterization. *Journal of Nanomaterials*, *2015*, 1–6.

Chen, Z., Yan, H., Liu, T., & Niu, S. (2016). Nanosheets of MoS2 and reduced graphene oxide as hybrid fillers improved the mechanical and tribological properties of bismaleimide composites. *Composites Science and Technology*, 2–3.

Chook, S. W., Chia, C. H., Zakaria, S., Ayob, M. K., Chee, K. L., & Huang, N. M. (2012). Antibacterial performance of Ag nanoparticles and AgGO nanocomposites prepared via rapid microwave-assisted synthesis method. *Nanoscale Research Letters*, *7*(1), 1.

Chung, I., Park, I., Seung-hyun, K., Thiruvengadam, M., & Rajakumar, G. (2016). Plant-Mediated Synthesis of Silver Nanoparticles : Their Characteristic Properties and Therapeutic Applications. *Nanoscale Research Letters*, 1.

Deng, L., Ouyang, X., Jin, J., Jiang, Y., Zheng, J., Li, J.,Yang, R. (2013). Exploiting the Higher Speci fi city of Silver Amalgamation: Selective Detection of Mercury(II) by Forming Ag/Hg Amalgam. *Analytical Chemistry*, (Ii), 1–7.

Ding, H., Zhang, S., Chen, J., Hu, X., Du, Z., Qiu, Y., & Zhao, D. (2015). Reduction of Graphene Oxide at Room Temperature. *Thin Solid Films*, 2–4.

Drewniak, Sabina, R. M. (2016). Studies of Reduced Graphene Oxide and Graphite. *Sensors*, 1–16.

Dubey, P., Kumar, A., & Prakash, R. (2015). Non-covalent Functionalization of Graphene Oxide by Polyindole and Subsequent Incorporation of Ag Nanoparticles for Electro-chemical Applications. *Applied Surface Science*, 3–4.

Ebrahimi, S. (2015). In fl uence of Stone – Wales defects orientations on stability of graphene nanoribbons under a uniaxial compression strain. *Solid State Communications*, *220*, 17–20.

Fan, L., Zhang, H., Zhang, P., & Sun, X. (2015). Applied Surface Science One-step synthesis of chlorinated graphene by plasma enhanced chemical vapor deposition. *Applied Surface Science*, *347*, 632–635.

Fu, C., Zhao, G., Zhang, H., & Li, S. (2013). Evaluation and Characterization of Reduced Graphene Oxide Nanosheets as Anode Materials for Lithium-Ion Batteries. *Electrochemical Science*, *8*, 6269–6280.

Gao, L., Lian, C., Zhou, Y., Yan, L., Li, Q., Zhang, C., Chen, K. (2014). Biosensors

and Bioelectronics Graphene oxide – DNA based sensors. *Biosensors and Bioelectronic*, *60*, 22–29.

Garima, Q. (2014). Journal of Industrial and Engineering Chemistry A review on carbon nanotubes and graphene as fillers in reinforced polymer nanocomposites. *Journal of Industrial and Engineering Chemistry*, 1–15.

Guy, O. J., & Walker, K. D. (2016). *Graphene Functionalization for Biosensor Applications*. *Silicon Carbide Biotechnology* (Second Edi). United Kingdom: Elsevier Inc.

Han, Y., Luo, Z., Yuwen, L., Tian, J., Zhu, X., & Wang, L. (2013). Applied Surface Science Synthesis of silver nanoparticles on reduced graphene oxide under microwave irradiation with starch as an ideal reductant and stabilizer. *Applied Surface Science*, *266*, 188–193.

Han, Y., Wang, T., Gao, X., Li, T., & Zhang, Q. (2016). Preparation of thermally reduced graphene oxide and the influence of its reduction temperature on the thermal , mechanical , flame retardant performances of PS nanocomposites. *Composites part A*, 3–4.

Ismagilov, R. (2013). *Formation of carbon nano- and micro-structures by chemical vapor deposition*. Finland: University of Eastern Finland.

Jin, Z., Owour, P., Lei, S., & Ge, L. (2015). Graphene, graphene quantum dots and their applications in optoelectronics. *Current Opinion in Colloid & Interface Science*, 3.

Jr, K. E. W., & Sheehan, P. E. (2014). Graphene Synthesis. *Diamond & Related Materials*, 1–22.

Kai-Chih Hsu, D.-H. C. (2014). Microwave-assisted green synthesis of Ag/reduced graphene oxide nanocomposite as a surface-enhanced Raman scattering substratewith high uniformity. *Nanoscale Research Letters*, 2.

Kamali, K. Z., Pandikumar, A., & Jayabal, S. (2015). Amalgamation based optical and colorimetric sensing of mercury (II) ions with silver @ graphene oxide nanocomposite materials. *Ag@GO Nanocomposite for Optical Detection of Hg(II)*, (Ii), 2–5.

Liu, L., Qing, M., Wang, Y., Chen, S., & Ph, D. (2015). Defects in Graphene: Generation, Healing, and Their Effects on the Properties of Graphene: A Review. *Journal of Materials Science & Technology*, 4–6.

Loh, K. P., Bao, Q., Eda, G., & Chhowalla, M. (2010). Graphene oxide as a chemically tunable platform for optical applications. *Nature Publishing Group*, *2*(12), 1015–1024.

Loryuenyong, V., Totepvimarn, K., Eimburanapravat, P., Boonchompoo, W., & Buasri, A. (2013). Preparation and Characterization of Reduced Graphene Oxide Sheets via Water-Based Exfoliation and Reduction Methods. *Advances in Materials Science and Engineering*, *2013*(2013), 1–6.

Mallakpour, S., Abdolmaleki, A., & Borandeh, S. (2015). Surface functionalization of GO, preparation and characterization of PVA/TRIS-GO nanocomposites. *Polymer*, 3.

Moraes, A., & Brandelli, A. (2016). Anti-adhesion and antibacterial activity of silver nanoparticles supported on graphene oxide sheets. *Colloids and Surface B : Biointerfaces*, (August 2013), 119.

Nersisyan, H. H., Kim, S. H., Lee, T. H., & Lee, J. H. (2014). Author â€™ s Accepted Manuscript. *Materials Letters*, 2–3.

Neto, A. H. C. (2009). The electronic properties of graphene. *Reviews of Modern Physics*, *81*(March), 110.

Noor, M., Rameshkumar, P., & Huang, N. M. (2015). Visual and spectrophotometric determination of mercury (II) using silver nanoparticles modified with graphene oxide, (Ii), 3.

Othman, M., Ritikos, R., Syed, H., Jaafar, M., Khanis, H., Maisarah, N., … Rahman, S. A. (2015). Low-temperature plasma-enhanced chemical vapour deposition of transfer-free graphene thin films. *Materials Letters*, 2–3.

Papailias, I., Giannouri, M., Trapalis, A., Todorova, N., Giannakopoulou, T., Boukos, N., & Lekakou, C. (2015). Decoration of crumpled rGO Sheets with Ag Nanoparticles by Spray Pyrolysis. *Applied Surface Science*, 2–4.

Ramesh, G. V, & Radhakrishnan, T. P. (2011). A Universal Sensor for Mercury (Hg , Hg I , Hg II) Based on Silver Nanoparticle-Embedded Polymer Thin Film. *Applied Materials and Interfaces*, 988–994.

Royal, T. H. E., Academy, S., & Sciences, O. F. (2010). Graphene. *The Royal Swedish Academy Of Sciences*, *50005*(October), 0–10.

Sahu, D., Sarkar, N., Sahoo, G., Mohapatra, P., & Swain, S. K. (2015). Silver Imprinted Graphene Nanocomposites : Synthesisis and Morphological Study, *1*(July), 224–227.

Scopel, W. L., Paz, W. S., & Freitas, J. C. C. (2016). Interaction between single vacancies in graphene sheet : An ab initio calculation. *Solid State Communications*, 1–2.

Shao, Y., Wang, J., Wu, H., Liu, J., Aksay, I. A., & Lin, Y. (2010). Graphene Based Electrochemical Sensors and Biosensors : A Review. *Electroanalysis*, 1027–1036.

Sharmila, T. K. B., Antony, J. V, Jayakrishnan, M. P., Beegum, P. M. S., & Thachil, E. T. (2015). Mechanical, thermal and dielectric properties of hybrid composites of epoxy and reduced graphene oxide/iron oxide. *JMADE*, 1–25.

Silwana, B., Horst, C. Van Der, & Iwuoha, E. (2015). Synthesis, characterisation and electrochemical evaluation of reduced graphene oxide modified antimony nanoparticles. *Thin Solid Films*, 1–53.

Singh, V., Joung, D., Zhai, L., Das, S., Khondaker, S. I., & Seal, S. (2011). Graphene based materials: Past, present and future. *Progress in Materials Science*, *56*(8), 1178–1271.

Sridhar, V., Lee, I., Yoon, H., Chun, H., & Park, H. (2013). Microwave synthesis of three dimensional graphene-based shell-plate hybrid nanostructures. *Carbon*, *61*, 633–639.

Sundaram R.S. (2014). *Graphene: Properties, Preparation, Characterisation and Devices*. (A. B. K. Viera Skakalova, Ed.). UK: Germany and University of Cambridge.

Tam, T. Van, Hur, S. H., Chung, J. S., & Choi, W. M. (2015). Ultraviolet light sensor based on graphene quantum dots / reduced graphene oxide hybrid film. *Sensors and Actuators A*, 3.

Thondaiman, M. (2015). Synthesis and Characterization of Mass Synthesis and Characterization of Mass production of high quality Reduced production of high quality Reduced Graphene Sheets via a a Chemical Method Graphene Sheets via Chemical Method. *Research Advances in Communication, Computation, Electrical Science and Structures*, 1–14.

Vermisoglou, E. C., Giannakopoulou, T., Romanos, G., Giannouri, M., Boukos, N., Lei, C., … Trapalis, C. (2015). Effect of hydrothermal reaction time and alkaline conditions on the electrochemical properties of reduced graphene oxide. *Applied Surface Science*, 1–31.

Wang, F., Drzal, L. T., Qin, Y., & Huang, Z. (2016). *Enhancement of fracture toughness, mechanical and thermal properties of rubber/epoxy composites by incorporation of graphene nanoplatelets*. *Composites part A*. Elsevier Ltd.

Xia, H., Zhang, X., Shi, Z., Li, Y., Wang, J., & Qiao, G. (2015). Mechanical and thermal properties of reduced graphene oxide reinforced aluminum nitride ceramic composites. *Materials Science & Engineering A*, 1–25.

Yavari, F., & Koratkar, N. (2012). Graphene-Based Chemical Sensors. *Physical Chemistry Letters*, 1746–1753.

Yin, Z., Wu, S., Zhou, X., Huang, X., Zhang, Q., & Boey, F. (2010). Electrochemical Deposition of ZnO Nanorods on Transparent Reduced Graphene Oxide Electrodes for Hybrid Solar Cells. *Small*, 307–312.

Zhang, B., Wang, Y., & Zhai, G. (2015). Biomedical applications of the graphene-based materials. *Materials Science & Engineering C*, 3–4.

Zhao, J., Zeng, H., Li, B., Wei, J., & Liang, J. (2015). Journal of Physics and Chemistry of Solids Effects of Stone-Wales Defect Symmetry on the Electronic Structure and Transport Properties of Narrow Armchair Graphene Nanoribbon. *Journal of Physical and Chemistry of Solids*, *77*, 8–13.

Zhuang Liu, Joshua T.Robinson, X. S. (2009). PEGylated Nano-Graphene Oxide for delivery of Water Insoluble Cancer Drugs. *J Am Chem Soc.*, *130*(33), 10876–10877.

APPENDIX A

EXPERIMENTAL METHOD

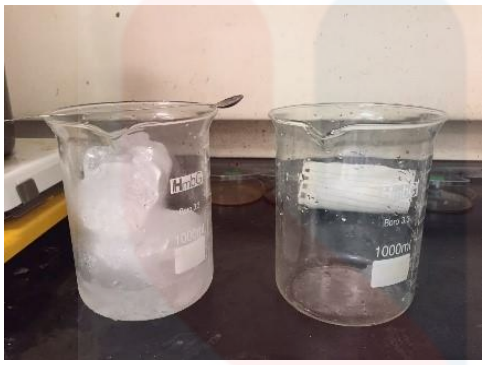

Figure A.1: The mixture of Ice and H_2O_2 .

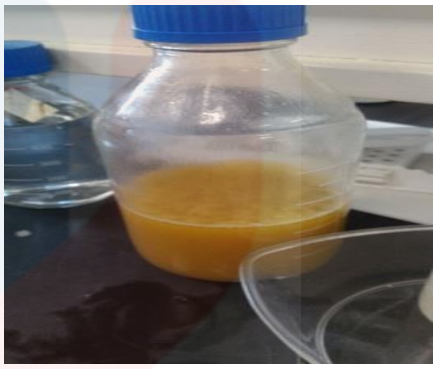

Figure A.2: The mixture of ice, H_2O_2 and mixture from step 1.

Figure A.3: After second washed.

Figure A.4: After third washed.

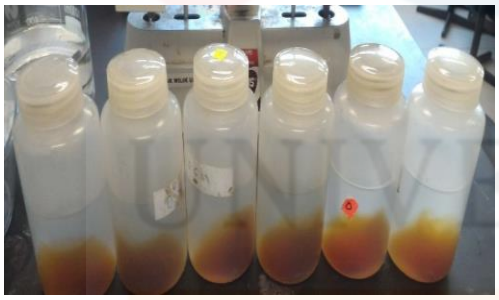

Figure A.5: After forth time washed.

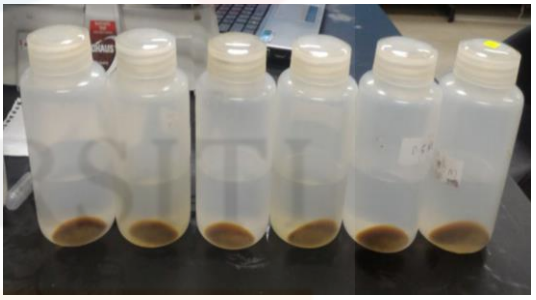

Figure A.6: After fifth time washed.

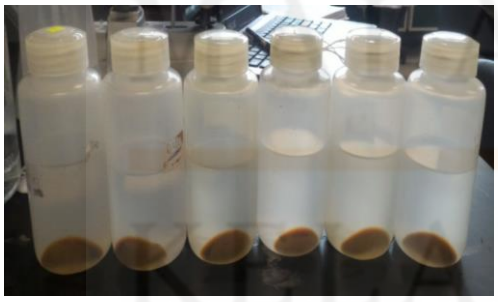

Figure A.7: After sixth time washed.

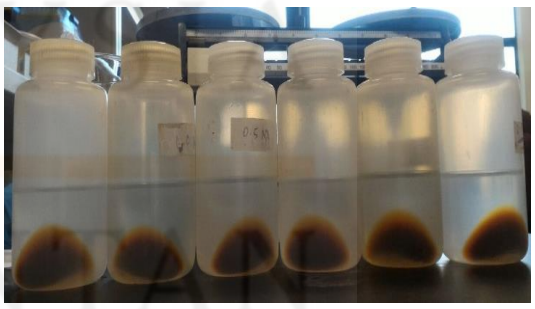

Figure A.8: After seventh time washed.

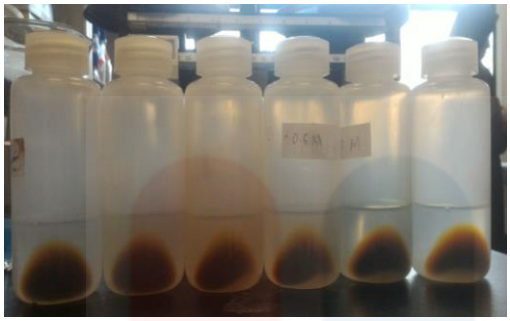

Figure A.9: After eighth time washed.

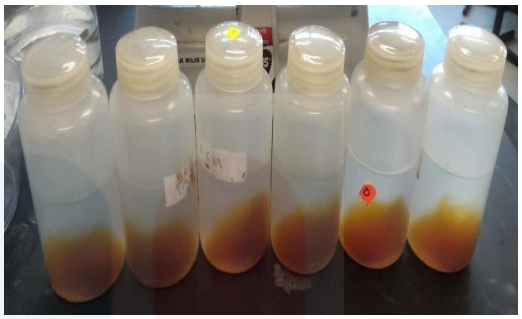

Figure A.10: After tenth time washed.

APPENDIX B

CALCULATION

B.1 Preparation of silver nitrate:

For 0.1 M $= \frac{(0.1)(10ml)(169)}{1000}$

= 0.169 gram

For 0.5 M = $\frac{(0.5)(10ml)(169)}{1000}$

= 0.845 gram

For 1.0 M = $\frac{(1.0)(10ml)(169)}{1000}$

= 1.69 gram (optimum weight of silver nitrate)

B.2 Preparation of HgCl (0.001M)

n = $\frac{mv}{1000}$

= $\frac{g}{jmr}$

g = $\frac{(0{,}001)(10ml)}{1000}$ x 271.52

= 0.027 g HgCl (into 10 ml of H_2O)

$V_2 = \frac{(1\mu M)(2mlG0 - Ag)}{0.001}$

= 200 µl

B.3 Synthesising of GO-Ag nanocomposite

To produce 0.1 mg/ml:

$M_1V_1 = M_2V_2$

$$V_1 = \frac{(0.1mg/ml)(50ml)}{(5mg/ml)}$$

= 1 ml (into 50 ml H_2O)

APPENDIX C

TABLES

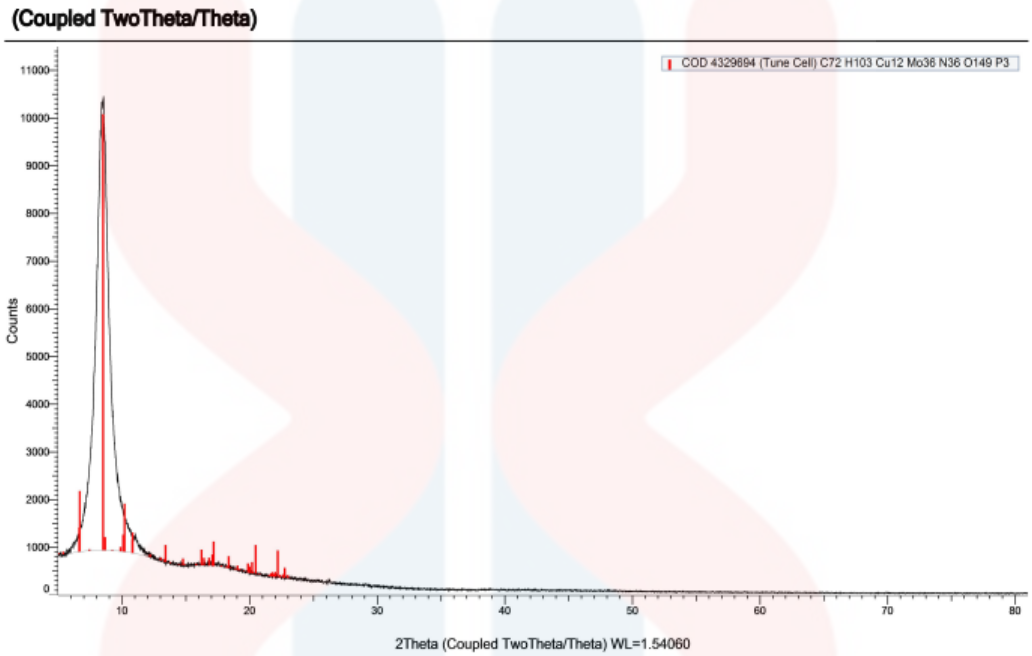

Figure C.1: XRD analysis of GO from EVA.

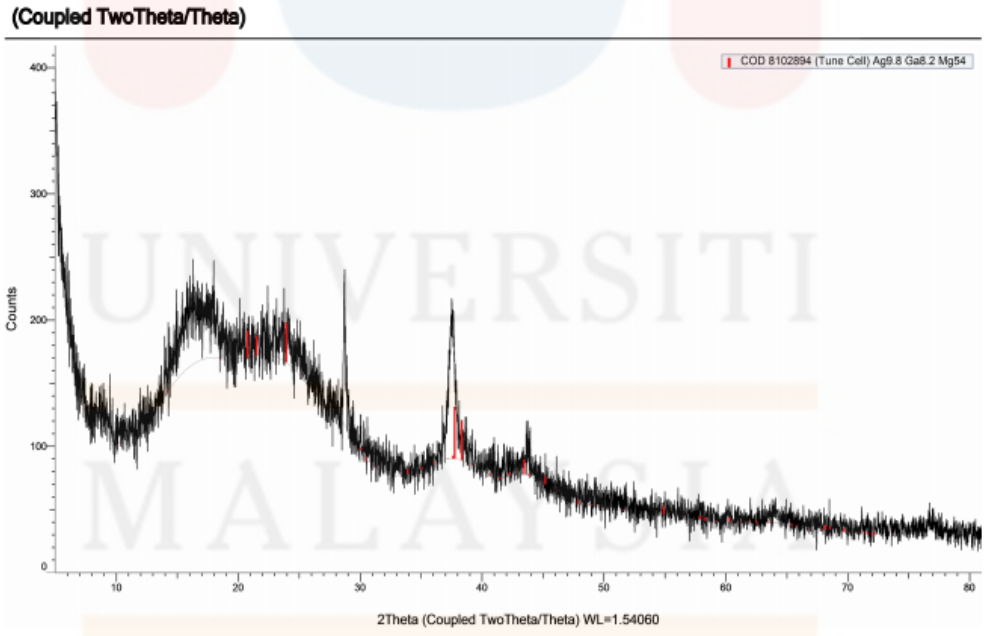

Figure C.2: XRD Analysis of GO-Ag from EVA.